Accepted Manuscript

An insight into the adsorption of diclofenac on different biochars: mechanisms, surface chemistry, and thermodynamics

Linson Lonappan, Tarek Rouissi, Satinder Kaur Brar, Mausam Verma, Rao Y. Surampalli

Please cite this article as: Lonappan, L., Rouissi, T., Kaur Brar, S., Verma, M., Surampalli, R.Y., An insight into the adsorption of diclofenac on different biochars: mechanisms, surface chemistry, and thermodynamics, *Bioresource Technology* (2017), doi: https://doi.org/10.1016/j.biortech.2017.10.039

An insight into the adsorption of diclofenac on different biochars: mechanisms, surface chemistry, and thermodynamics

Linson Lonappan[a], Tarek Rouissi[a], Satinder Kaur Brar[a]*, Mausam Verma[b], Rao Y. Surampalli[c]

[a]INRS-ETE, Université du Québec, 490, Rue de la Couronne, Québec, Canada G1K 9A9

[b]CO$_2$ Solutions Inc., 2300, rue Jean-Perrin, Québec, Canada G2C 1T9

[c]Department of Civil Engineering, University of Nebraska-Lincoln, N104 SEC P.O. Box

886105, Lincoln, NE 68588-6105, United States

(*Corresponding author, Phone: +1 418 654 3116; Fax: +1 418 654 2600;

E-mail: satinder.brar@ete.inrs.ca)

Abstract

Biochars were prepared from feedstocks pinewood and pig manure. Biochar microparticles obtained through grinding were evaluated for the removal of emerging contaminant diclofenac (DCF) and the underlying mechanism were thoroughly studied. Characterization of biochar was carried out using particle size analyzer, SEM, BET, FT-IR, XRD, XPS and zeta potential instrument. Pig manure biochar (BC-PM) exhibited excellent removal efficiency (99.6%) over pine wood biochar (BC-PW) at 500 µg L^{-1} of DCF (environmentally significant concentration). Intraparticle diffusion was found to be the major process facilitated the adsorption. BC-PW

1

followed pseudo first-order kinetics whereas BC-PM followed pseudo second –order kinetics. Pine wood biochar was largely affected by pH variations whereas for pig manure biochar, pH effects were minimal owing to its surface functional groups and DCF hydrophobicity. Thermodynamics, presence of co-existing ions, initial adsorbate concentration and particles size played substantial role in adsorption. Various isotherms models were also studied and results are presented.

Keywords: diclofenac; adsorption; biochar; interface chemistry; thermodynamics; mechanisms

1. Introduction

Emerging contaminants (ECs) are gaining wider attention nowadays due to their potential environmental impacts. Even though ECs are detected at fairly low concentrations, the adverse effects of ECs on several organisms are high and usually uncertain for several ECs. Among the emerging contaminants, pharmaceutical, diclofenac (DCF) is often detected in wastewater treatment plant influent, effluent, surface water and drinking water (Farré et al., 2008; Heberer, 2002; Stuart et al., 2012). It is estimated that about 1443 ± 58 tons of DCF are consumed globally on an annual basis (Acuña et al., 2015), which makes it as the 12th bestselling generic molecule globally worth $1.61\pm 15\%$ billion sales per year (Palmer, 2012). This large consumption, in turn, resulted in the ubiquitous presence of DCF in wastewater. The incomplete degradation of DCF in wastewater treatment plants leads to its presence in surface water and even in drinking water (Vieno & Sillanpää, 2014). This presence in water resources causes toxic concerns towards several aquatic and terrestrial organisms (Lonappan et al., 2016a). It has been reported that even at 250 ng L^{-1}, DCF can induce tissue damages in several mussel species and

2

at 1 μg L^{-1}, cytological alterations in rainbow trout (Ericson et al., 2010).Thus, even very small concentrations of DCF can lead to a considerable effect on the aquatic ecosystems.

In the recent decades, adsorption has emerged as an effective treatment method for the removal of various organic emerging contaminants, such as pharmaceuticals (Nam et al., 2014; Westerhoff et al., 2005). Activated carbons from the various origin are the conventional adsorbents studied for the removal of ECs (Westerhoff et al., 2005). The physicochemical properties of adsorbents and adsorbates, such as, hydrophobicity, surface functional groups, pore size, external surface area and chemical composition determine the removal efficiency along with other experimental parameters, such as pH and temperature (Lonappan et al., 2016c; Nam et al., 2014; Nielsen et al., 2014). However, all adsorbents even after surface activation cannot become excellent adsorbents for all contaminants. For instance, most of the activated carbons will exclude larger molecules (>3000 Da) due to its small pore size (<2 nm) (Kilduff et al., 1996). Moreover, the activation process is an additional procedure and incurs a cost. Thus, economical and eco-friendly adsorbents must be specifically identified for the compounds of interest to be treated. As a waste management alternative, carbonaceous material biochar exhibited its potential towards sustainability and demonstrated its usefulness as a value-added product for several environmental applications (Glaser et al., 2009; Lonappan et al., 2016c; Woolf et al., 2010). Biochar is carbon negative (Glaser et al., 2009) material and hence the production and consumption are appealing towards a sustainable future. For biochar, the adsorption mechanisms and adsorption capacity significantly vary with feedstock and method of production as a result of changes in the chemical properties and surface chemistry. Pinewood and pig manure are two of the largest produced agricultural and farming industry residues in Quebec, Canada; which needed proper recycling/disposal. Hence, production of biochar from these

3

materials is an excellent waste management and valorization alternative. Moreover, biochars of this category are well known for its richness in micropores and adsorption abilities (Lonappan et al., 2016c). The porous structure and surface chemistry features make biochar an excellent adsorbent for several environmental contaminants. Due to the aromaticity and hydrophobicity, biochar is an excellent sorbent for a number of hydrophilic organic compound and inorganic compounds(Fang et al., 2014). A proper understanding of the interactions between adsorbate and adsorbent is necessary to design efficient adsorption systems for the removal of contaminants.

The aim of this study is to evaluate the adsorption efficiency and adsorption processes of two carbonaceous materials; biochar derived from pinewood and pig manure for the removal of a model emerging contaminant, DCF for the first time. Biochar microparticles were prepared and characterized by particle size analyzer, scanning electron microscope, Fourier transform infrared spectroscopy, X-ray diffraction and Brunauer, Emmett and Teller (BET) analysis and zeta potential instrument. The underlying sorption processes, such as adsorption rate, adsorption model, and adsorbent/adsorbate interaction were studied using equilibrium adsorption data by various kinetic and isotherm models. The effect of adsorbent dosage, particle size and thermodynamic behavior of adsorption were also studied. Moreover, the effect of surface charges on adsorption was studied by pH variations and zeta potential measurements. The result presented explains the effect of feedstock, chemical and surface features of biochar for the effective removal of DCF.

2. Material and methods

2.1. Materials

Pinewood biochar sample (BC- PW) was obtained from Pyrovac Inc. (Quebec, Canada). BC-PW was derived from pine white wood (80% v/v) purchased from Belle-Ripe in Princeville and the rest was spruce and fir (20%). BC-PW was produced at $525\pm1°C$ under atmospheric pressure for 2 minutes in the presence of nitrogen (to create oxygen free environment) and used as obtained from the reactor outlet. The second biochar sample prepared from pig manure (BC-PM) was obtained from "Research and Development Institute for Agri-Environment" (IRDA), Quebec, Canada. BC-PM was derived from the solid fraction of pig slurry and prepared at 400 ± 1 °C for 2 h at $15°C$ min^{-1} in the presence of nitrogen at a flow rate of 2 L min^{-1} during heating. Powdered activated carbon (AC) was used as positive control for the adsorption studies to compare the adsorption results and was purchased from Fisher scientific (Ottawa, Canada). At a time about 200 grams of raw biochar samples was used for microparticle production. Samples were ground using 'Retsch RS 200' vibratory disc mill at 750 rpm for 2 minutes for BC-PW and 1 minute for BC-PM. Subsequently, the obtained particles were sieved through ASTM 200 numbered sieve (corresponds to less than 75µm particle size) for 10 minutes. The particle size and size distribution were further confirmed using Horiba particle size analyzer (LA-950 Laser Particle Size Analyzer, Horiba, Japan).

Diclofenac sodium salt (98%; CAS 15307-79-6) was purchased from Fisher Scientific (Ottawa, ON, Canada). An internal standard (IS), diclofenac-d_4 was obtained from C/D/N isotopes Inc. (Montreal, QC, Canada). The molecular weight of diclofenac is 296.14864 g/mol. Other properties are: log K_{ow} = 4.51 and pK_a = 4.15.

All the experiments were carried out using Milli-Q water (18 MΩ cm^{-1} at 25 °C) and were prepared in the laboratory using Milli-Q/Milli-RO Millipore system (Milford, MA, USA). All the reagents used for analysis of DCF and for pH adjustment of samples were of analytical grade.

5

2.2 Methods

2.2.1 Physico-chemical properties of microparticles

Horiba particle size analyzer was used to measure the particle size distribution of microparticles. The analysis was carried out in duplicate and the mean value was measured. Surface characteristics of prepared microparticles were investigated by EVO® 50 smart scanning electron microscope (SEM) (Zeiss, Germany). Specific surface area was obtained from Brunauer, Emmett and Teller (BET) N_2 adsorption isotherms at 77 K (Autosorb-1, Quantachrome, USA). The presence of functional groups on the surface of adsorbents was investigated by Fourier transform infrared spectroscopy (FT-IR; Perkin Elmer, Spectrum RXI, FT-IR instrument fitted with lithium tantalate (LiTaO$_3$) detector. Powder x-ray diffraction (XRD) patterns of the samples were recorded using Panalytical Empyrean XRD with monochromatized CuK alfa radiation (1.5418 A). The surface charge properties of adsorbents were investigated by zeta potential measurements, which were conducted at a different equilibrium pH using a Nano-ZS Zetasizer (Malvern Instruments Inc., UK). Samples were pre-equilibrated to different pH (2, 5, 7, 10 and 13) maintaining a constant biochar dosage of 2 g L^{-1}. The zeta potential was measured in duplicate at each pH and the mean was calculated.

2.2.2 Batch adsorption studies

Batch adsorption studies were carried out in 125 mL conical flasks with 50 ml of sample in an INFORS HT - multitron standard shaking incubator (INFORS, Mississauga, Canada). The agitation was carried out at 200 rpm and kept constant throughout the study. The temperature was set to be 25 ±1°C and 0.1g of biochar was used for the study at pH 6.5 (unless stated otherwise for a particular study). Prior to analysis, the biochar samples were dried overnight at

6

60 ±1°C in an oven and then cooled in a desiccator to remove any moisture present. After adsorption, DCF samples were separated using centrifugation at 11600 x g for 10 minutes in a MiniSpin® plus centrifuge. Post centrifugation, the supernatant was analyzed for DCF left in the liquid.

The adsorption capacity at time t (in µg g^{-1}) was calculated using Equation 1:

$$q_t = V(C_0 - C_t)/w$$ -- (1)

Percentage of DCF removal at time 't' was calculated using Equation 2

$$\% \, removal \, (\%R) = \left\{ \left(\frac{C_0 - C_e}{C_0} \right) 100 \right\}$$-------------------------------------- (2)

Where C_0, C_t and C_e represent the concentrations of DCF (mg L^{-1}) at the beginning of the experiment, at time t (min), and at equilibrium respectively; V is the volume of the solution used for the study (L); and w is the mass of biochar used (g).

2.2.3 Equilibrium and kinetics of adsorption

Equilibrium adsorption studies were carried out for 2 mg L^{-1} of DCF for 48 h. Sampling was carried out each hour for the first 12 hours and then for each 6-hour interval untilthe end of the experiment (48 h). The data was used to study the kinetics and equilibrium of adsorption for BC-PW and BC-PM. For this study, pH was kept constant at 6.5 and temperature was maintained at 25°C.

Adsorption process (adsorption rate, model, and information about adsorbent/adsorbate interaction - physisorption or chemisorption) was evaluated by Pseudo-first-order rate equation,

7

Pseudo-second-order rate equation and Elovich equation. The theory behind each equation is given in supplementary information (SI).

2.2.4 Varying DCF concentrations and adsorption isotherms

Adsorption studies were carried out using 0.1 g of biochar microparticles concentrations varied from 0.1 mg L^{-1} to 10 mg L^{-1} (0.1, 0.25, 0.5, 1, 3, 5 and 10 mg L^{-1}). The pH was kept constant at 6.5 and temperature was maintained at 25°C. Equilibrium data were used to study the adsorption isotherm models. Langmuir, Freundlich, Temkin, and Dubinin- Radushkevich (D-R) isotherm models were used to study the adsorption process. The theory behind each model is given in supplementary information (SI)

2.2.5 pH and adsorption

Adsorption studies were carried out at different pH, 2, 6.5, 10, and 12.5 to evaluate the effect of varying pH on adsorption. In this experiment, studies were carried out using 1 mg L^{-1} of DCF prepared in milli-Q water. The pH of biochar samples was analyzed using an independent method (Nielsen et al., 2014). In short, biochar samples were added to milli-Q water containing DCF and the pH of the sample was adjusted using 1N NaOH or HCl. Adsorption experiments were carried out until reaching equilibrium and samples were analyzed for zeta potential and DCF.

2.2.6 Thermodynamics of adsorption

The thermodynamics of adsorption of DCF on BC-PW and BC-PM was evaluated by carrying out adsorption study at 10°C, 20°C, 25°C, 30°C, 40°C and 50°C with 500 μg L^{-1} of DCF. The study on the effect of temperature on adsorption will extend the knowledge of thermodynamic

parameters, such as Gibbs free energy of adsorption (ΔG°), heat of the adsorption (ΔH°) and standard entropy changes (ΔS°) (Suriyanon et al., 2013). Thermodynamic equations used for these calculations are given in Equations 3 and 4:

$$\ln\left(\frac{q_e}{c_e}\right) = \frac{\Delta S^{\circ}}{R} - \frac{\Delta H^{\circ}}{RT} \quad \text{-- (3)}$$

$$\Delta G^{\circ} = \Delta H^{\circ} - T\Delta S^{\circ} \quad \text{-- (4)}$$

Where R is the universal gas constant (8.314 J mol^{-1} K^{-1}) and T is the absolute temperature in Kelvin (K). ΔH° and ΔS° can be determined from the slope and intercept of the plots between $ln\left(q_e/c_e\right)$ versus 1/T (equation 13). ΔG° can be calculated from equation 4.

2.2.7 Microparticles and adsorption

To study the effect of adsorption on biochar microparticles in comparison with raw biochar (as obtained from: millimeters to high micrometers range) adsorption studies were carried out using biochar as obtained. According to the International Union of Pure and Applied Chemistry (IUPAC) guidelines (terminology for biorelated polymers and applications (IUPAC Recommendations, 2012), microparticles are defined as particles with dimensions between 1×10^{-7} and 1×10^{-4} m. The preparation technique for microparticles is described in section 2.1. The behavior of microparticles is unique since microparticles have a larger surface-to-volume ratio than the macroscale. For further comparison activated carbon was used as a positive control for this study.

2.2.8 DCF analysis

Stock solutions of diclofenac and diclofenac-d$_4$ (1 g L^{-1}) were prepared in methanol and stored in amber colored bottles at 4±1 °C, until use. All the reagents used for analysis of DCF are of

9

analytical grade. Laser diode thermal desorption tandem mass spectroscopy (LDTD- MS/MS) was used for the analysis of DCF samples(Lonappan et al., 2016b). The instrument comprised LDTD-APCI (Laser diode thermal desorption - atmospheric pressure chemical ionization) source (LDTD T-960, Phytronix Technologies, Quebec, Canada) mounted on a TSQ Quantum access triple quadruple mass spectrometer (Thermo Scientific, Mississauga, Ontario, Canada).

3 Results and discussion

3.1 Physico-chemical properties of biochar

Scanning electron micrographs of biochar (Fig.1 in (Lonappan et al., 2017) and supplementary file) showed rough and uneven surfaces with the presence of several pores. For both C-PM and BC-PW, as per visual image data, pores are of the dimensions of micrometers (μm). For BC-PW, pores are well arranged whereas, for BC-PM, the pores are unevenly distributed. However, these micro and macro pores facilitate the adsorption of DCF having a molecular size in A° dimension(Jung et al., 2015).

The Brunauer, Emmett, and Teller (BET) specific surface area of raw pine wood biochar (BC-PW-R) was fairly very small at 0.18 m^2 g^{-1}, whereas with microparticles of pinewood biochar (BC-PW-M) an increase in surface area (13.3 m^2 g^{-1}; about 75-fold) was observed. For raw pig manure biochar (BC-PM-R) surface area was 21.4 m^2 g^{-1} and with microparticles (BC-PM-M), it was increased to 43.5 m^2 g^{-1} (Nielsen et al., 2014). Thus, size reduction resulted in an increased surface area and this has been discussed in a previous study (Lonappan et al., 2016c). The surface area of activated carbon used was 900 m^2 g^{-1}. Other properties, such as ash content and moisture content which can affect adsorption properties are already given in a previous publication(Lonappan et al., 2016c).Fourier transform infra-red (FTIR) spectra was recorded for

both BC-PW and BC-PM (Fig. 2 in (Lonappan et al., 2017) and supplementary file). For pinewood biochar (BC-PW), wood cellulose is a polymer rich material with hydroxyl groups and even after pyrolysis, some hydroxyl moiety remains in the sample (Chia et al., 2012) and a sharp and medium peak near 3400 cm^{-1} indicated the presence of O-H stretching in the plane with a free hydroxyl group. A medium and narrow peak at 2912 cm^{-1} showed the presence of alkanes with C-H stretching. The narrow peak at 2362 cm^{-1} was identified as the presence of nitrile group (C≡N). Since BC-PW is derived from a plant source, the presence of lignin/cellulose-derived transformation products was observed (Keiluweit et al., 2010) (multiple peaks starting around 1600 cm^{-1} to 700 cm^{-1}). A strong, but narrow peak at 1584 cm^{-1} was due to aromatic ring modes which is characteristic for chars derived from lignocellulose materials, such as pinewood (softwood) (Sharma et al., 2004). A medium peak at 1373 cm^{-1} was attributed to the presence of alkane (C-H) bending. A strong peak at 1197 cm^{-1} was due to sulfonic acids with S=O stretching. A peak at 873 cm^{-1} could be due to C-H bending (1, 2, 4-trisubstituted) and a medium peak at 812 cm^{-1} signified aromatic C-H bending (trisubstituted). Moreover, a medium peak at 750 cm^{-1} was due to aromatic C-H bend (out of the plane). The FTIR spectra of pig manure biochar (BC-PM) revealed their complex functional groups consisting of a mixture of mineral and organic matter. Generally, biochar from pig manure feedstock consists of several inorganic functional groups, such as metals(Zhang et al., 2013). For pig manure biochar, a narrow peak at 3400 cm^{-1} was identified as N-H stretch which could be due to the presence of secondary amines. The narrow peak at 2533 cm^{-1} showed the presence of mercaptans (S-H stretch). A broad and strong peak of around 1422 cm^{-1} is due to the C–C stretch (in the –ring) which confirmed the presence of aromatics. The broad and strong peak around 1114 cm^{-1} was due to C-O stretch and pointed towards the presence of carboxylic acid functional groups. Since

11

pig manure is rich in phosphorus, a peak around 874 cm^{-1} and 563 cm^{-1} can be assigned to PO_4^{3-} group. The peak of around 712 cm^{-1} could be due to the presence of calcium and peak around 617 cm^{-1} was assigned to the presence of disulfides (S-S) stretching since pig manure is rich in minerals. Moreover, peak around 563 cm^{-1} was assigned to the presence of alkyl halides.

X-ray diffraction (XRD) analysis was conducted for BC-PW and BC-PM to study the crystallinity behaviour of the biochar (Fig. 3 in (Lonappan et al., 2017) and supplementary file). The chemical structure of the adsorbent plays a key role in the interaction between adsorbent and adsorbate and hence explains adsorption potential and mechanism. For BC-PW, distinct peaks of around 25 and 44, 2θ° angle were attributed to the presence of quartz (Zhang et al., 2015).

Particle size distribution of the prepared microparticles is given in Fig 1. The particle size distribution was well within the defined microparticles range with a diameter of less than 100 μm. The mean particle size of pig manure biochar microparticle (BC-PM) was observed to be ≈30.6 μm with 9.32 μm, 22.52 μm and 61.58 μm for D10 (particle diameter corresponding to 10% cumulative (from 0 to 100%) undersize particle size distribution), D50 (particle diameter corresponding to 50% cumulative (from 0 to 100%) undersize particle size distribution) and D90(particle diameter corresponding to 90% cumulative (from 0 to 100%) undersize particle size distribution) values, respectively.

3.2 Microparticles and adsorption

Removal efficiencies of raw biochar, biochar microparticles and activated carbon under different concentrations and at an initial hour and at equilibrium time is given in Fig.2. Adsorption studies were focused on environmentally relevant concentrations of DCF such as 500 μg L^{-1}. Pinewood biochar as obtained- (BC-PW-R) showed the lowest removal efficiency for DCF at 10 mg L^{-1}

12

and 500 µg L^{-1}. For both concentrations, the maximum removal efficiency was obtained at equilibrium which was reached after 4.5 hours. The maximum removal efficiency obtained was 40 % for BC-PW-R, whereas as with pine wood biochar microparticles (BC-PW-M), this removal efficiency was enhanced to 68% and which was obtained for 500 µg L^{-1} of DCF at equilibrium. This enhancement in removal efficiency is attributed towards the increase in surface area from 0.18 m^2 g^{-1} to 13.3 m^2 g^{-1} which provided an increase in adsorption sites. Moreover, DCF being a molecule with a negative charge; will be drawn towards the positive charges on the biochar surface. Functional groups, such as a free hydroxyl group will create positive surface radicals on biochar that will assist in the overall adsorption of DCF.

Biochar derived from pig manure exhibited higher adsorption potential and hence higher removal efficiency over pine wood biochar. Even raw pig manure biochar (as obtained form) (BC-PM – R) exhibited good removal efficiency of 61.8 % in the first hour of adsorption and which increased up to 80.8% at equilibrium at 10 mg L^{-1} DCF. Moreover, at an environmentally relevant concentration of 500 µg L^{-1}, the maximum removal efficiency obtained was 82%. With pig manure biochar microparticles (BC-PM-M), the removal efficiency was enhanced up to 98% and 99.6%, respectively at 10 mg L^{-1} and 500 µg L^{-1} and at equilibrium. This excellent removal efficiency of pig manure biochar can be attributed to its surface area: 21.4 m^2 g^{-1} for raw biochar and 43.5 m^2 g^{-1} for microparticles. The increase in removal efficiency of microparticles (BC-PM-M) was due to the availability of higher surface area for adsorption through size reduction. Moreover, FTIR analysis proved the presence of inorganic surface functional groups and metals in pig manure biochar. Presence of a variety of surface functional groups, such as halides, sulfides, carboxylic acids, phosphates along with other organics enhanced the adsorption potential. Previous studies also reported the specific ability of pig manure-derived biochar for the

removal of herbicides (Zhang et al., 2013). Furthermore, it is to be noted that at an environmentally relevant concentration, pig manure-derived biochar microparticles exhibited removal efficiency near 100% (99.6 %) at equilibrium. Commercially available activated carbon was effective at 10 mg L^{-1} DCF owing to its much larger surface area. In addition, activated carbon exhibited its potential for rapid adsorption so that equilibrium was attained in less than one hour with excellent removal efficiency (99.4 %). However, at lower concentration (500 µg L^{-1}), the removal efficiency was 95% for activated carbon even after 5 hours of contact time. For biochar microparticles derived from pig manure, the removal efficiency increased to 99.6% at equilibrium. Hence, pig manure biochar can be used as an effective adsorbent for micropollutants and as a potential replacement for activated carbon.

Apart from the enhanced surface area, several other factors influenced and increased adsorption potential/ removal efficiency of pig manure biochar in comparison with biochar derived from pine wood. Previous molecular modeling studies reported the interactions between DCF and biochar surfaces (Jung et al., 2015). In addition, depending upon the type of the adsorption, several interactions, such as p-p electron donor-acceptor interactions, hydrophobic interactions, hydrogen bonding and Van der Waal forces are involved in adsorption. The larger molecular butterfly structure of DCF(Jung et al., 2015; Lonappan et al., 2016b) maximizes the p-p interactions between the surface of biochar and DCF (Schames et al., 2004). The structure comprising one aromatic ring will be always parallel to the adsorbent and other will be perpendicular and which will enhance the interaction with biochar surface making DCF always available for biochar. In this study, biochar derived from pig manure and pinewood is rich in organic functional groups evident from the available FTIR results. The aromatic carbon will enhance the hydrophobic interactions owing to its component ratio (Chen et al., 2007; Jung et al.,

14

2015). Also, the effect of the copious presence of non-aromatic carbon, aliphatic carbon, and other inorganic functional groups in pig manure biochar cannot be overruled. The interactions between polarizable biochar surfaces will act as electron donors and polar aromatic DCF (electron acceptors) can also be expected (Chen et al., 2007). Hence, these interactions with aromatic groups in addition to inorganic functional groups make pig manure biochar a better adsorbent for DCF over pine wood biochar. Moreover, these enhanced interactions due to the presence of a large variety of inorganic and organic functional groups could be the reason for enhanced adsorption potential for pig manure biochar at lower concentrations in comparison with activated carbon despite lower surface area.

Co-existing ion effect also had a considerable effect on adsorption of DCF onto biochar. Zhang et al,2013 reported that presence of metals, such as Ca and Mg can enhance DCF adsorption (Zhang et al., 2013) by forming DCF- metal precipitates or complexes. Elemental and metal analysis (supplementary data) showed that Mg (mg/kg) (PM- 10111.52±78.6, PW- 143.45±10.2) and Ca (PM- 45481.88±26.8 and PW- 1753.38±14.5) concentrations are much higher in PM than PW and thus formed precipitates which in turn resulted in enhanced adsorption by BC-PM. Moreover, XPS analysis has been conducted to confirm co-existing ion effect as well as further confirm the results obtained from FTIR.

From XPS results, it is evident that the presence of other ions, such as metals enhanced the adsorption potential of BC-PM. Detailed report on XPS analysis has been provided as supplementary information. For pinewood biochar, the fit is not perfect with the function used for the asymmetry, but as expected the main peak is highly asymmetrical and its width is very small; it can be shown that the π-π^* satellite has an intensity only between 2.6 and 4.6% of the total C1s intensity, it is located at around 6 eV on the high BE side of the main peak and has a

15

width larger than 2eV. As there are no contaminants on this sample, especially oxygen, there are no peaks associated with carbon-oxygen bonds.

For pig manure biochar, O1 and C1 spectrums showed the presence of various impurities and metal oxides. Moreover, C=O and C-O bonding were predominant in these samples. 2p Ca was also observed that can directly influence the DCF adsorption through metal complexation of DCF with Ca.

3.3 Equilibrium studies and kinetic models

The equilibrium time was determined based on adsorption studies on biochar microparticles across time. Results showed that equilibrium was reached after 4.5 hours for BC-PW and after 5 hours for BC-PM. The initial rapid adsorption for both biochars facilitated a rapid adsorption to reach equilibrium. Moreover, nature and available sorption sites of adsorbents affected the adsorption equilibrium (Bhattacharya et al., 2008).

Adsorption kinetic models can predict chemical reactions, reaction rate, and particle diffusion mechanism of DCF onto biochar microparticles. However, elementary kinetic models, such as first and second order rate equations are not applicable to the adsorption system with solid surfaces, such as biochar, which are rarely homogeneous since the effects due to chemical reactions involved and the transport phenomena are often experimentally inseparable (Sparks, 1989). In this study, pseudo first-order, pseudo second-order, Elovich l and the intra-particle diffusion models were used. Results (Table 1) showed that kinetics of DCF adsorption onto biochar microparticles were correlated with the linear forms of these four models. Kinetic equations and theoretical aspects involved in the models are given in supplementary information.

16

For BC-PW, all the studied models exhibited a good correlation with the experimental data (correlation coefficients obtained were 0.93, 0.99 and 0.95 respectively for pseudo first-order, the pseudo-second-order and Elovich kinetic). However, even with a correlation coefficient near to unity, pseudo-second order failed to obtain a theoretical equilibrium concentration from a model which was equal or comparable with the experimentally observed equilibrium concentration. With a correlation coefficient of 0.938, calculated equilibrium concentration was comparable with experimentally observed equilibrium concentration in pseudo-first-order model. Elovich model also gave a better fitting to the experimental data with a correlation coefficient of 0.95. However, the pseudo first-order model was selected as the model for the adsorption DCF on BC-PW due to its excellent agreement with the experimental equilibrium concentration value. Hence during adsorption mass transfer from the bulk to the adsorption sites are occurred driving and the driving force is the concentration difference (Lagergren, 1898; Smith et al., 2016). Thus, the concentration of DCF in the bulk solution played a significant role in the adsorption of DCF on to BC-PW.

For BC-PM, correlation coefficients of 0.937, 0.9915 and 0.970 were observed for pseudo first-order, pseudo second-order and Elovich kinetic model respectively. Moreover, equilibrium concentration calculated from pseudo-second order was in better agreement with the observed experimental equilibrium concentration with a percent error of less than 5%. Thus the adsorption kinetics of BC-PM was better explained by pseudo-second-order kinetic model. As a result, chemical reaction/ chemisorption can be assumed as the rate controlling step for the adsorption process(Smith et al., 2016). A chemical reaction involving the strong complexation of DCF with the active sites on the BC-PM took place during adsorption. Moreover, pseudo second-order suggests the rate of adsorption for BC-PM is dependent on the availability of the sorption sites

17

rather than the concentration of the DCF in the bulk solution (Liu, 2008). The Elovich model gives also a better fitting to the experimental data with a correlation coefficient of 0.97 indicates that chemisorption is a dominant process during adsorption and suggesting heterogeneous adsorption (Low, 1960).

Both BC-PM and BC-PW exhibited good agreement with the intraparticle diffusion model and hence for both samples mechanism of adsorption can be explained on the basis of intraparticle diffusion. However, for intraparticle diffusion mechanism was not the rate-determining step since the intercept did not cross the origin in the IPD curve(Dural et al., 2011)(data not shown).

3.4 Adsorption isotherm modeling

The adsorption isotherm explains about the interactions between DCF and the biochar microparticles and consequently the adsorption mechanisms. Theoretical aspects regarding adsorption isotherms and the isotherm plots are given as supplementary data. Isotherm data obtained for different adsorption isotherm models for both BC-PW and BC-PM is given in Table 2. BC-PW followed the Langmuir adsorption isotherm model with $R^2 = 0.984$ and hence homogeneous monolayer adsorption onto the surface can be expected (Tan et al., 2009). Thus no re-adsorption to the surface is taking place during the adsorption. Temkin ($R^2 = 0.92$) and Dubinin- Radushkevich (D-R) ($R^2 = 0.73$) isotherm models were not linearly fitting the experimental data and thus were not considered. However, Freundlich isotherm model resulted in R^2 of 0.94. Even though, owing to higher R^2 obtained with Langmuir isotherm model and a Q_0 (μg g-1) of 526.3 which was almost equal to the Q_0 observed in actual experimental conditions, Langmuir isotherm model has been thus selected as the best fitting model. Hence, a maximum adsorption capacity of 526.3 μg g^{-1} can be observed at 500 μg L^{-1} of DCF through isotherm

18

models. Moreover, Langmuir isotherm model rate of adsorption has been calculated as 1.39 x 10^{-3} L μg^{-1} (Kilduff et al., 1996; Tan et al., 2009).

BC-PM followed the Freundlich isotherm model (R^2 = 0.99) which involved multilayer adsorption. All the other models (Langmuir, Temkin, and D-R) resulted in poor R^2 with the experimental values (Table 1). Thus, the stronger binding sites on the surface are occupied first and that the binding strength decreased with the increasing degree of site occupancy and which reduced the adsorption with time. Hence, after an initial increase in adsorption capacity, adsorption decreased gradually due to unavailability of adsorption sites (Freundlich, 1906; Tan et al., 2009). Moreover, Freundlich isotherm model suggested the possibility of heterogeneous multilayer adsorption involving binding by both physical and chemical forces. However, the high value of n (favourability factor for heterogeneity; 1/n = 0.87) ruled out the possibility of heterogeneity in this study.

3.5 pH effect on adsorption of DCF

Effect of pH on adsorption is an important parameter to study as adsorption is being a surface controlled process. The pH of BC-PW was found to be 8.5 and 11.22 for BC-PM. Thus, negative surface charges are predominant on the surface of biochar. Fig.3 demonstrated a correlation between pH, zeta potential and the adsorption of DCF on biochar. For BC-PW and BC-PM, higher adsorption occurred at acidic pH. Moreover, BC-PW was significantly affected by pH (88.6±2 % at pH 2 to 36±3 % at pH 12.5) as compared to BC-PM (about 99.8 ± 2 % at pH 2 to 88.8 ± 2 % at pH 12.5) for removal efficiency of DCF. Furthermore for both biochars removal was always favored by acidic pH.

19

Ionizable micropollutants can interact with adsorbents through electrostatic attraction or repulsion, and this interaction varied depending on their pKa values (Huerta-Fontela et al., 2011). DCF is considered as a weak acid as its pKa is around 4.15 (Nam et al., 2014). For hydrophobic compounds such as DCF, the adsorption could be largely affected by the pH changes. Hence, electrostatic and specific sorbate-sorbent interactions (based on surface polarities, functional groups, organic and inorganic components of biochars)(Nielsen et al., 2014) between DCF and biochar surface do have an impact on adsorption.

The isoelectric point (pH$_{IEP}$) of BC-PW was calculated to be 2.45 from zeta potential - pH curve (Fig 3). Excellent removal efficiency (88.6 %) and hence adsorption was exhibited by BC-PW at acidic pH. DCF being a negative ion at acidic pH higher adsorption can be expected. Consequently, at acidic pH and even pH near to pH$_{IEP}$, excellent removal was obtained. This phenomenon can be explained on the basis of electrostatic attraction between negatively charged DCF and positive biochar surface. Further, removal efficiency was decreased by 60% with an increase in pH. The electrostatic interactions played a major role in the adsorption of DCF onto BC-PW microparticles. Adsorption of DCF onto BC-PW was mainly due to physical forces of attraction which may include electrostatic interactions, Van der Waals forces, and hydrophobic interactions. In addition, both the biochar and DCF are hydrophobic in nature and this factor might have facilitated the adsorption and favorable pH. Excellent adsorption near to (pH$_{IEP}$) is suggested the possibility of other mechanisms involved in the adsorption process. This can be attributed to H- bonding possibility with oxygen-containing groups, such as OH$^-$ on the surface of biochar (Fang et al., 2014; Nam et al., 2015) along with hydrogen bonding with other aromatic functional groups, such as aromatic C-H which are observed on the surface of biochar.

20

The isoelectric point (pH_{IEP}) of BC-PM was calculated to be 2.15 from zeta potential - pH curve. For BC-PM, the adsorption was also pH dependent, the maximum removal efficiency (99.8%) was observed at pH of 2; while it decreased to 88.8% at pH 12.5. This decrease could be due to the changes in the surface charge and hence the negative surface of biochar repelled DCF anion. However, in comparison with BC-PW, the drastic decrease in removal efficiency was minimum and even at unfavorable pH of 12.5; 88.8% of removal efficiency was observed. Physical processes, such as electrostatic interactions are not the major process involved in the adsorption DCF onto BC-PM. The removal process can be explained on the basis of electrostatic interactions, H- bonding, hydrophobic effects, and π–π EDA interactions. The presence of oxygen-containing functional groups, such as carboxylic acids facilitated the adsorption through H- bonding irrespective of pH (Fang et al., 2014). Moreover, polar functional groups, such as hydroxyl and amine groups exhibited electron-withdrawing effect at basic pH values(Ji et al., 2010) and these groups can interact with aromatic rings (π electron acceptors) in BC-PM. Minerals and inorganic functional groups, such as disulfides and halides are present in BC-PM and has positively affected the adsorption, irrespective of the pH.

3.6 Thermodynamics of DCF adsorption

Adsorption studies were carried out at various temperatures: 10°C, 20°C, 25°C, 30°C, 40°C and 50°C. Thermodynamic parameters were calculated according to equations (13) and (14). Different behaviors were observed for BC-PW and BC-PM with adsorption along with temperature (Table 3). In the liquid phase adsorption, the adsorption of adsorbate occurred while solvent species were

removed from the sorption sites. Displacement enthalpies are the key factors in this process as they balance different weak interactions between adsorbent, adsorbate, and solvent.

The thermodynamic factors affecting the adsorption process are summarized in Table 3. For BC-PW, a decrease in adsorption capacity ($\mu g\ g^{-1}$) was observed along with an increase in temperature. An adsorption capacity of 141.82 $\mu g\ g^{-1}$ was observed at 10° C (283K) and which decreased along with an increase in temperature to 75.34 $\mu g\ g^{-1}$ at 50° C (323K) under equilibrium conditions. Previously, similar results were observed for diclofenac adsorption on Isabel grape bagasse (Antunes et al., 2012) and for the removal of other pharmaceuticals on carbon black(Cuerda-Correa et al., 2010). In these studies, authors explained this phenomenon based on two processes: the energy exchange between sorbate, sorbent and the solvent and the solubility of pharmaceuticals. Elevated temperatures can increase the solubility of the pharmaceutical; hence in a better soluble condition, pharmaceuticals will have a higher affinity towards the solvent than the adsorbent. In addition, along with temperature, vapor pressure also increased and density of the adsorbate decreased which will decrease the adsorption as a result of decreased interactions between DCF and biochar surface (BC-PW). For BC-PW, adsorption was endothermic ($\Delta H°$ =1.130 KJ mol^{-1}) Moreover, 1.130 KJ mol^{-1} for $\Delta H°$ indicated that the process is physisorption since the adsorption energies for physisorption are lower than 40 KJ mol^{-1}. A negative value of $\Delta S°$ (-4.40 J mol^{-1} K^{-1}) suggested that randomness at the solid –solution interface decreased during the adsorption. The possible reason could be the formation of more than one layer of adsorption (Antunes et al., 2012). Also, the total process was non-spontaneous ($\Delta G°$= positive). A similar behavior was observed in a previous study as well for dye adsorption onto activated bentonite(Özcan & Özcan, 2004). For DCF adsorption, a similar behaviour was observed with adsorption of DCF on to Isabel grape bagasse (*Vitis labrusca*)(Antunes et al.,

22

2012). The positive value and thus non-spontaneity of the process could be due to the presence of energy barrier which hindered the adsorption process. This could be due to the repulsive electric charges (negative) (Antunes et al., 2012; Özcan & Özcan, 2004) which were present on the surface of biochar. Adsorption of DCF on BC-PW was highly pH dependent (section 3.5) and electrostatic attraction forces played a major role in the adsorption and hence thermodynamic behaviour of DCF adsorption onto BC-PW is in good agreement with the observations made using pH variable study.

A completely different behavior was obtained for BC-PM, a small increase in adsorption capacity ($\mu g\ g^{-1}$) was observed along with an increase in temperature. An adsorption capacity of 236.53 $\mu g\ g^{-1}$ was observed at 10° C (283K) and which increased along with an increase in temperature to 247 $\mu g\ g^{-1}$ at 50° C (323K). Thus, the effect of temperature on adsorption was minimal. This increase can be attributed to increased surface coverage of DCF at higher temperature due to the expansion and creation of new active sites on BC-PM. The larger size of DCF and the possible presence of metal oxide catalysts (creates active sites at a higher temperature, identified by FTIR) in BC-PM could be the reason for slightly better adsorption at higher temperatures. For BC-PM, a value of $\Delta H° = -3.970$ KJ mol^{-1} suggests adsorption process as exothermic. A positive value of $\Delta S°$ (16.13) suggested that randomness at the solid-liquid interface increased during the adsorption. The whole process was spontaneous; indicated by a negative $\Delta G°$ value. Similar results for spontaneity have been reported for adsorption of anti-inflammatory pharmaceutical naproxen on activated carbon (Önal et al., 2007)

4. Conclusions

23

The adsorption of DCF onto BC-PM was found to be effective over BC-PW. About 99.6% removal efficiency was observed for BC-PM at an environmentally relevant concentration of 500 μg L^{-1}. For BC-PW, adsorption was explained by pseudo first-order model whereas for BC-PM by pseudo second-order model. For both adsorbents, intraparticle diffusion was found to be the major mechanism explaining the adsorption behavior. BC-PW adsorption was largely affected by the pH, whereas pH dependency of adsorption of BC-PM was minimal. Thermodynamic behavior of both adsorbents suggested adsorption of DCF on BC-PW was endothermic while exothermic for BC-PM.

E-supplementary data for this work can be found in e-version of this paper online.

References

24

Acuña, V., Ginebreda, A., Mor, J.R., Petrovic, M., Sabater, S., Sumpter, J., Barceló, D. 2015. Balancing the health benefits and environmental risks of pharmaceuticals: Diclofenac as an example. *Environ. Int.* 85, 327-333.

Antunes, M., Esteves, V.I., Guégan, R., Crespo, J.S., Fernandes, A.N., Giovanela, M. 2012. Removal of diclofenac sodium from aqueous solution by Isabel grape bagasse. *Chem. Eng. J.* 192, 114-121.

Bhattacharya, A.K., Naiya, T.K., Mandal, S.N., Das, S.K. 2008. Adsorption, kinetics and equilibrium studies on removal of Cr(VI) from aqueous solutions using different low-cost adsorbents. *Chem. Eng. J.* 137(3), 529-541.

Chen, W., Duan, L., Zhu, D. 2007. Adsorption of polar and nonpolar organic chemicals to carbon nanotubes. *Environ. Sci. Technol.* 41(24), 8295-8300.

Chia, C.H., Gong, B., Joseph, S.D., Marjo, C.E., Munroe, P., Rich, A.M. 2012. Imaging of mineral-enriched biochar by FTIR, Raman and SEM–EDX. *Vib. Spectrosc* 62, 248-257.

Cuerda-Correa, E.M., Domínguez-Vargas, J.R., Olivares-Marín, F.J., de Heredia, J.B. 2010. On the use of carbon blacks as potential low-cost adsorbents for the removal of non-steroidal anti-inflammatory drugs from river water. *J. Hazard. Mater.* 177(1–3), 1046-1053.

Dural, M.U., Cavas, L., Papageorgiou, S.K., Katsaros, F.K. 2011. Methylene blue adsorption on activated carbon prepared from Posidonia oceanica (L.) dead leaves: Kinetics and equilibrium studies. *Chem. Eng. J.* 168(1), 77-85.

Ericson, H., Thorsen, G., Kumblad, L. 2010. Physiological effects of diclofenac, ibuprofen and propranolol on Baltic Sea blue mussels. *Aquat Toxicol* 99(2), 223-31.

Fang, Q., Chen, B., Lin, Y., Guan, Y. 2014. Aromatic and hydrophobic surfaces of wood-derived biochar enhance perchlorate adsorption via hydrogen bonding to oxygen-containing organic groups. *Environ. Sci. Technol.* 48(1), 279-288.

Farré, M.l., Pérez, S., Kantiani, L., Barceló, D. 2008. Fate and toxicity of emerging pollutants, their metabolites and transformation products in the aquatic environment. *TrAC, Trends Anal. Chem.* 27(11), 991-1007.

Freundlich, H.M.F. 1906. Uber die adsorption in lasungen. *Z Phys Chem* 57, 385–470.

Glaser, B., Parr, M., Braun, C., Kopolo, G. 2009. Biochar is carbon negative. *Nature Geosci* 2(1), 2-2.

Heberer, T. 2002. Tracking persistent pharmaceutical residues from municipal sewage to drinking water. *Journal of Hydrology* 266(3), 175-189.

Huerta-Fontela, M., Galceran, M.T., Ventura, F. 2011. Occurrence and removal of pharmaceuticals and hormones through drinking water treatment. *Water Res.* 45(3), 1432-1442.

Ji, L., Liu, F., Xu, Z., Zheng, S., Zhu, D. 2010. Adsorption of pharmaceutical antibiotics on template-synthesized ordered micro- and mesoporous carbons. *Environ. Sci. Technol.* 44(8), 3116-3122.

Jung, C., Boateng, L.K., Flora, J.R.V., Oh, J., Braswell, M.C., Son, A., Yoon, Y. 2015. Competitive adsorption of selected non-steroidal anti-inflammatory drugs on activated biochars: Experimental and molecular modeling study. *Chem. Eng. J.* 264, 1-9.

Keiluweit, M., Nico, P.S., Johnson, M.G., Kleber, M. 2010. Dynamic molecular structure of plant biomass-derived black carbon (biochar). *Environ. Sci. Technol.* 44(4), 1247-1253.

Kilduff, J.E., Karanfil, T., Chin, Y.-P., Weber, W.J. 1996. Adsorption of natural organic polyelectrolytes by activated carbon: a size-exclusion chromatography study. *Environ. Sci. Technol.* 30(4), 1336-1343.

Lagergren, S. 1898. About the theory of so-called adsorption of soluble substances. *Kungliga Svenska Vetenskapsakademiens. Handlingar* 24(4), 1-39.

Liu, Y. 2008. New insights into pseudo-second-order kinetic equation for adsorption. *Colloids Surf. Physicochem. Eng. Aspects* 320(1–3), 275-278.

Lonappan, L., Brar, S.K., Das, R.K., Verma, M., Surampalli, R.Y. 2016a. Diclofenac and its transformation products: Environmental occurrence and toxicity - A review. *Environ. Int.* 96, 127-138.

Lonappan, L., Pulicharla, R., Rouissi, T., Brar, S.K., Verma, M., Surampalli, R.Y., Valero, J.R. 2016b. Diclofenac in municipal wastewater treatment plant: quantification using laser diode thermal desorption—atmospheric pressure chemical ionization—tandem mass spectrometry approach in comparison with an established liquid chromatography-electrospray ionization–tandem mass spectrometry method. *J. Chromatogr. A* 1433, 106-113.

Lonappan, L., Rouissi, T., Brar, S.K., Verma, M., Surampalli, R.Y. 2017. Adsorption of diclofenac onto different biochar microparticles : data set-characterization and dosage of biochar *Data in Brief* Submitted

Lonappan, L., Rouissi, T., Das, R.K., Brar, S.K., Ramirez, A.A., Verma, M., Surampalli, R.Y., Valero, J.R. 2016c. Adsorption of methylene blue on biochar microparticles derived from different waste materials. *Waste Manage. (Oxford)* 49, 537-544.

Low, M.J.D. 1960. Kinetics of Chemisorption of Gases on Solids. *Chem. Rev.* 60(3), 267-312.

Nam, S.-W., Choi, D.-J., Kim, S.-K., Her, N., Zoh, K.-D. 2014. Adsorption characteristics of selected hydrophilic and hydrophobic micropollutants in water using activated carbon. *J. Hazard. Mater.* 270, 144-152.

Nam, S.-W., Jung, C., Li, H., Yu, M., Flora, J.R.V., Boateng, L.K., Her, N., Zoh, K.-D., Yoon, Y. 2015. Adsorption characteristics of diclofenac and sulfamethoxazole to graphene oxide in aqueous solution. *Chemosphere* 136, 20-26.

Nielsen, L., Biggs, M.J., Skinner, W., Bandosz, T.J. 2014. The effects of activated carbon surface features on the reactive adsorption of carbamazepine and sulfamethoxazole. *Carbon* 80, 419-432.

Önal, Y., Akmil-Başar, C., Sarıcı-Özdemir, Ç. 2007. Elucidation of the naproxen sodium adsorption onto activated carbon prepared from waste apricot: Kinetic, equilibrium and thermodynamic characterization. *J. Hazard. Mater.* 148(3), 727-734.

Özcan, A.S., Özcan, A. 2004. Adsorption of acid dyes from aqueous solutions onto acid-activated bentonite. *J. Colloid Interface Sci.* 276(1), 39-46.

Palmer, E.,2012. Top 20 generic molecules worldwide. in: *Fiercepharma- Special report*, Vol. 2016, FierceMarkets, pp. special report.

Schames, J.R., Henchman, R.H., Siegel, J.S., Sotriffer, C.A., Ni, H., McCammon, J.A. 2004. Discovery of a novel binding trench in HIV integrase. *J. Med. Chem.* 47(8), 1879-1881.

Sharma, R.K., Wooten, J.B., Baliga, V.L., Lin, X., Geoffrey Chan, W., Hajaligol, M.R. 2004. Characterization of chars from pyrolysis of lignin. *Fuel* 83(11–12), 1469-1482.

Smith, Y.R., Bhattacharyya, D., Willhard, T., Misra, M. 2016. Adsorption of aqueous rare earth elements using carbon black derived from recycled tires. *Chem. Eng. J.* 296, 102-111.

Sparks, D.L. 1989. Application of chemical kinetics to soil chemical reactions. in: *Kinetics of Soil Chemical Processes*, Academic Press. San Diego, pp. 4-38.

Stuart, M., Lapworth, D., Crane, E., Hart, A. 2012. Review of risk from potential emerging contaminants in UK groundwater. *Sci. Total Environ.* 416, 1-21.

Suriyanon, N., Punyapalakul, P., Ngamcharussrivichai, C. 2013. Mechanistic study of diclofenac and carbamazepine adsorption on functionalized silica-based porous materials. *Chemical Engineering Journal* 214, 208-218.

Tan, I.A., Ahmad, A.L., Hameed, B.H. 2009. Adsorption isotherms, kinetics, thermodynamics and desorption studies of 2,4,6-trichlorophenol on oil palm empty fruit bunch-based activated carbon. *Journal of hazardous materials* 164(2-3), 473-82.

Vieno, N., Sillanpää, M. 2014. Fate of diclofenac in municipal wastewater treatment plant — A review. *Environ. Int.* 69, 28-39.

Westerhoff, P., Yoon, Y., Snyder, S., Wert, E. 2005. Fate of endocrine-disruptor, pharmaceutical, and personal care product chemicals during simulated drinking water treatment processes. *Environ. Sci. Technol.* 39(17), 6649-6663.

Woolf, D., Amonette, J.E., Street-Perrott, F.A., Lehmann, J., Joseph, S. 2010. Sustainable biochar to mitigate global climate change. *Nat Commun* 1, 56.

Zhang, J., Lü, F., Zhang, H., Shao, L., Chen, D., He, P. 2015. Multiscale visualization of the structural and characteristic changes of sewage sludge biochar oriented towards potential agronomic and environmental implication. *Sci. Rep.* 5, 9406.

Zhang, P., Sun, H., Yu, L., Sun, T. 2013. Adsorption and catalytic hydrolysis of carbaryl and atrazine on pig manure-derived biochars: Impact of structural properties of biochars. *J. Hazard. Mater.* 244–245, 217-224.

27

Figures – descriptions

Figure 1: Particle size distribution of biochar microparticles

Figure 2: Biochar microparticles and diclofenac removal efficiency (BC-PW-R: raw pinewood biochar, BC-PW-M : pinewood biochar microparticles, BC-PM-R : raw pig manure biochar, BC-PM-M : pig manure biochar microparticles, AC : activated carbon)

Figure 3: Effect of pH and zeta potential on removal efficiency of diclofenac (1 mg L^{-1} concentration); BC-PW: pine wood biochar, BC-PM: pig manure biochar

28
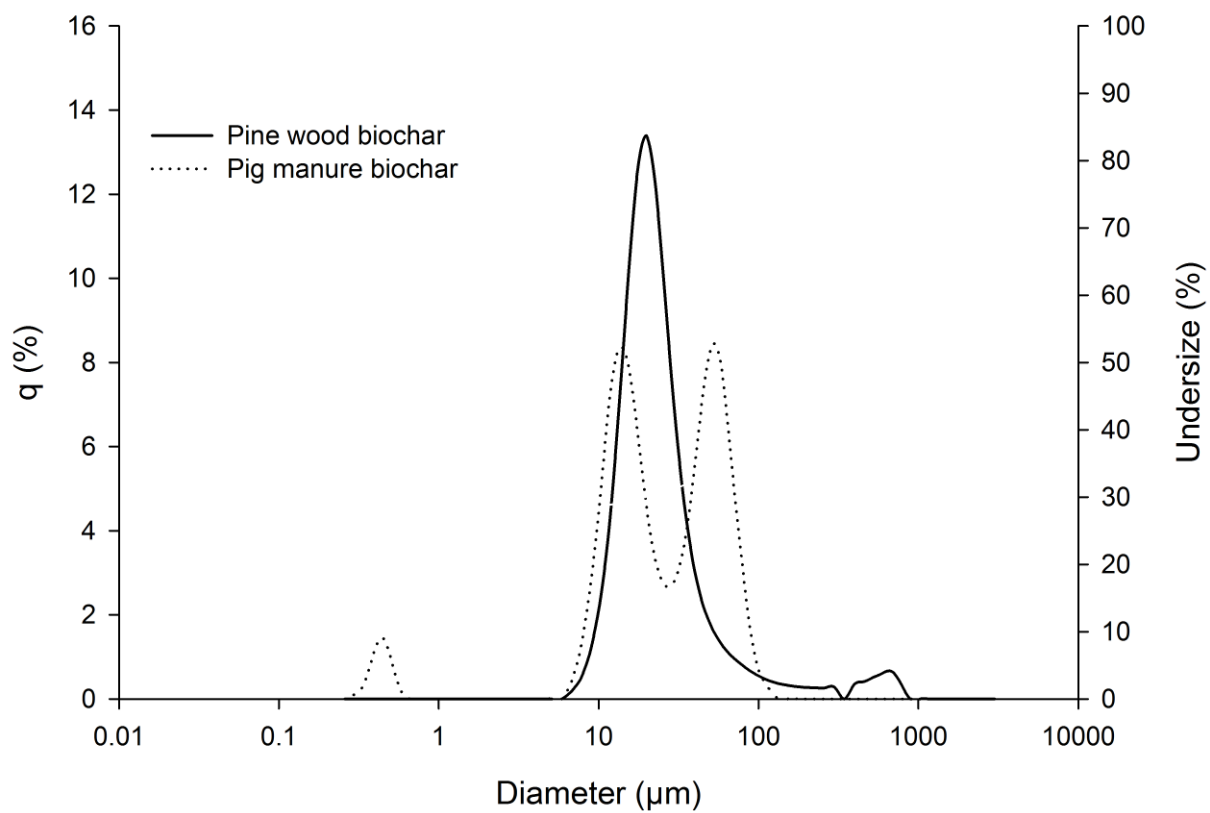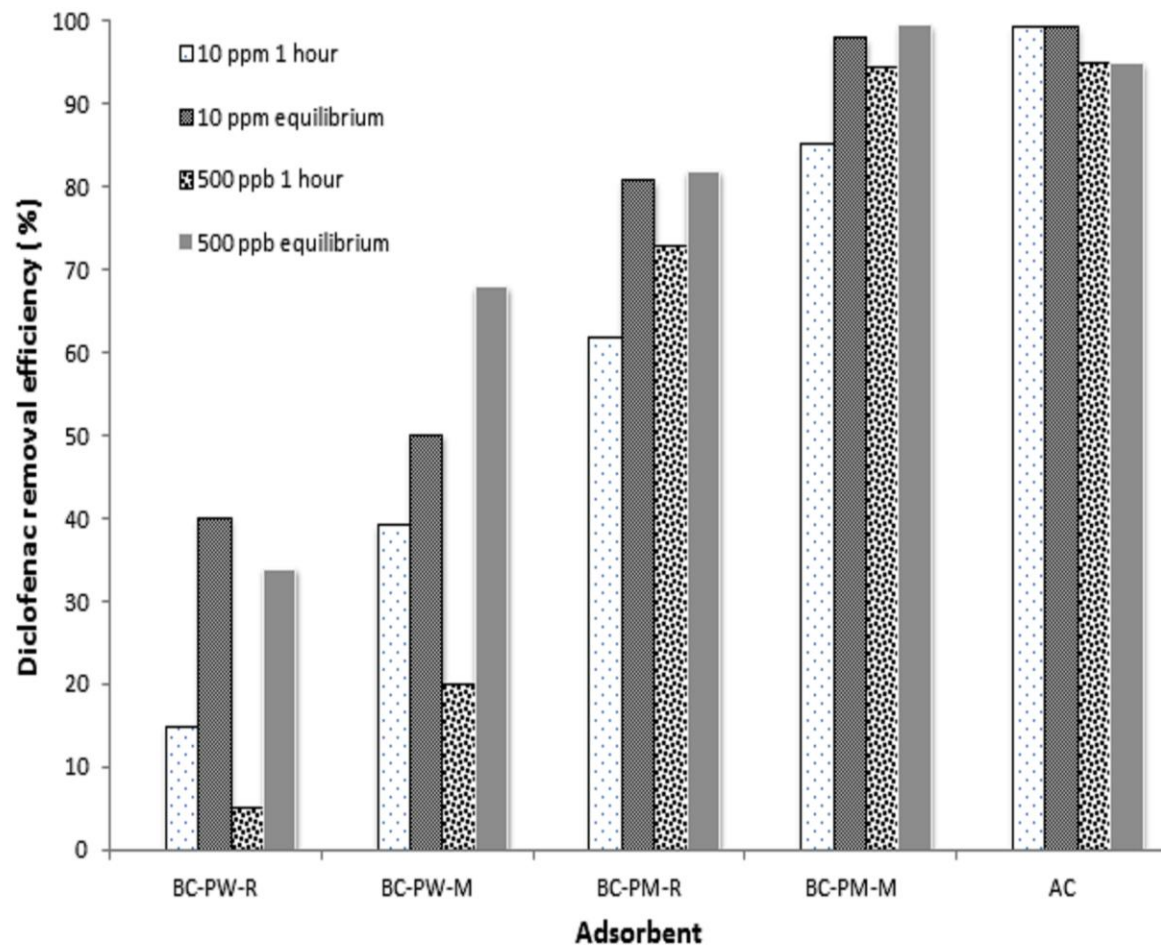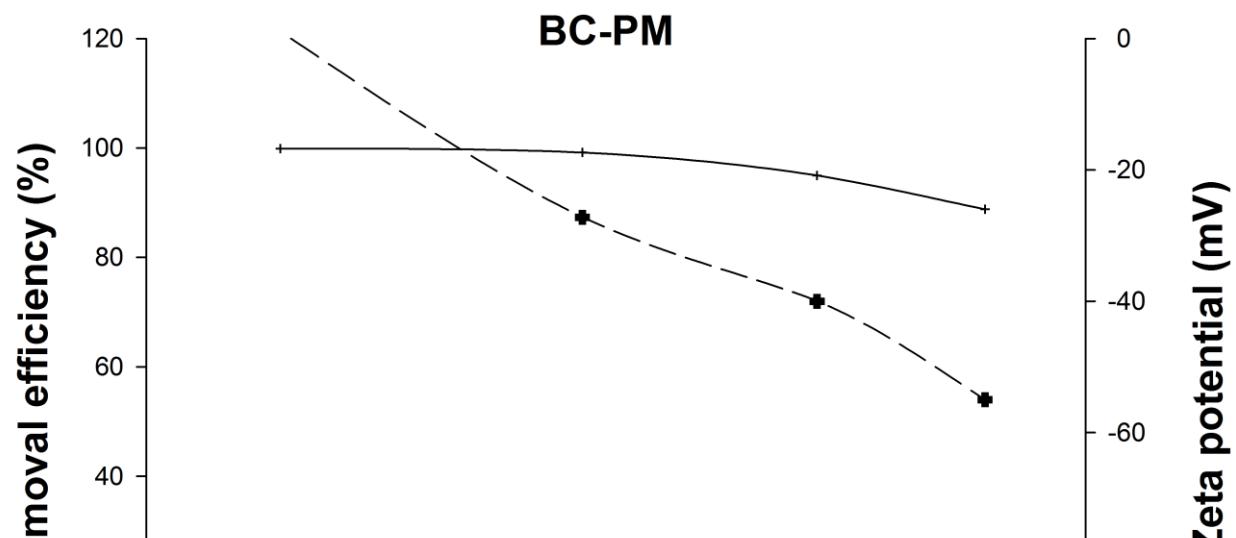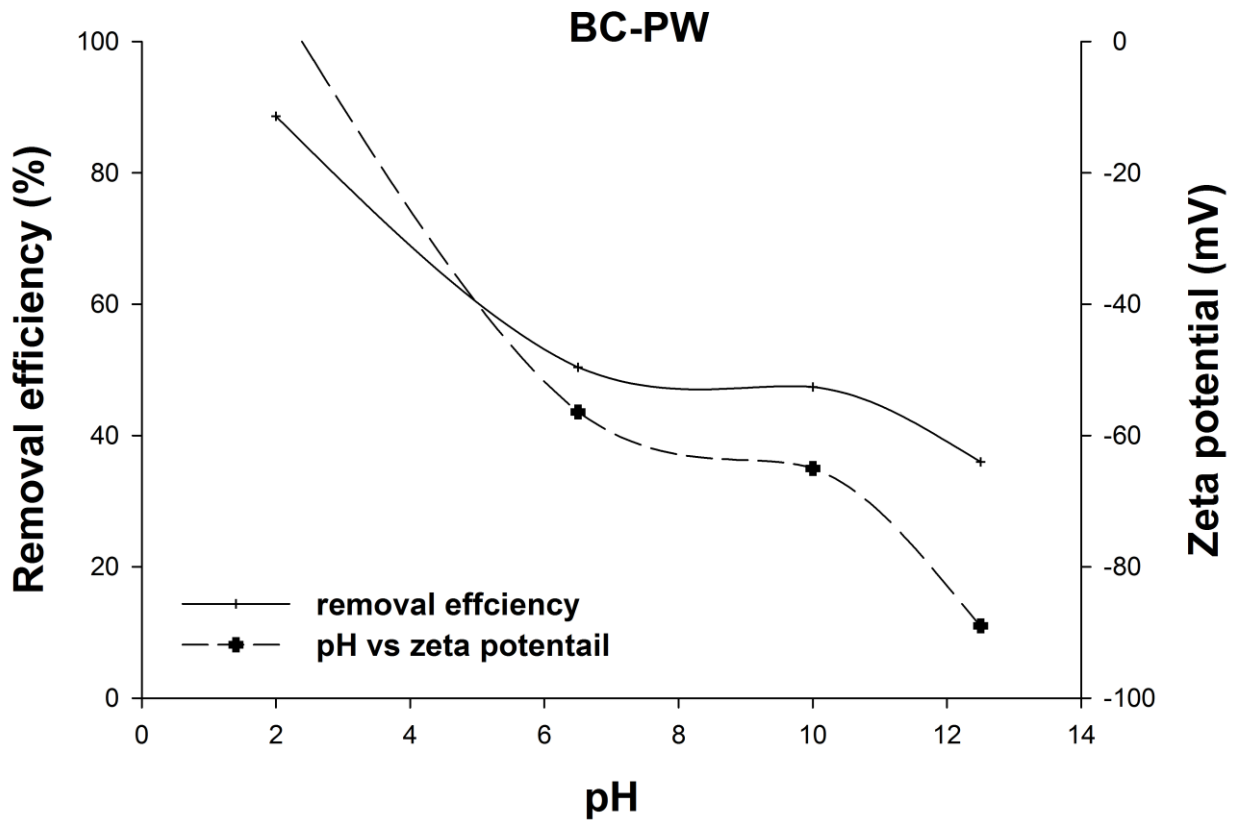
Tables

Micro-particle sample	q_e, experimental ($\mu g\ g^{-1}$)	Pseudo-first order model			Pseudo-second order model			Elovich model			Intraparticle diffusion model	
		q_e, cal. ($\mu g\ g^{-1}$)	k_1 (min^{-1})	R^2	q_e, cal. ($\mu g\ g^{-1}$)	K_2 ($g\ \mu g^{-1}\ min^{-1}$)	R^2	α ($\mu g\ g^{-1}\ min^{-1}$)	β ($g\ \mu g^{-1}$)	R^2	k_{id} ($\mu g\ g^{-1}min^{-1/2}$)	R^2
BC-PW	331	339.7	0.0133	0.938	400	3.82×10^{-5}	0.992	13.87	0.0117	0.9597	38.40	0.982
BC-PM	955	480.83	0.0175	0.937	1000	4.40×10^{-5}	0.991	5.07×10^{6}	0.0179	0.970	674.5	0.977

Table 1: Kinetic parameters for the adsorption of DCF onto biochar microparticles, BC-PW and BC-PM

*BC-PW: Pine wood biochar microparticles, BC-PM: Pig manure biochar microparticles

q_e and q_t are adsorbed ($\mu g\ g^{-1}$) DCF on biochar at equilibrium and at time t (min) respectively and k_1 is the rate constant of adsorption (min^{-1}). k_2 ($g\ \mu g^{-1}\ min^{-1}$) is the adsorption rate constant of pseudo-second-order adsorption process. α is the initial sorption rate ($\mu g\ g^{-1}\ min^{-1}$) and β is the desorption constant ($g\ \mu g^{-1}$). k_{id} ($\mu g\ g^{-1}min^{-1/2}$) is the intra-particle diffusion rate constant obtained from the intercept.

Table 2: Isotherm parameters adsorption of DCF onto biochar microparticles, BC-PW and BC-PM at equilibrium conditions

Micro-particle sample	Langmuir isotherm model			Freundlich isotherm model			Temkin isotherm model				Dubinin- Radushkevich (D-R) isotherm model			
	Q_0 ($\mu g\ g^{-1}$)	K_L ($L \mu g^{-1}$)	R^2	K_F ($\mu g\ g^{-1}$)	n	R^2	A_T ($L \mu g^{-1}$)	b_T	B	R^2	q_m ($\mu g\ g^{-1}$)	β ($mol^2 kJ^{-2}$)	E ($kJ\ mol^{-1}$)	R^2
BC-PW	526.3	1.39×10^{-3}	0.984	6.774	1.919	0.939	0.027	27.63	89.64	0.924	236.27	0.0005	0.0316	0.735
BC-PM	12500	8.47×10^{-4}	0.891	16.61	1.145	0.995	0.035	2.023	1224.4	0.878	2184.18	0.0002	0.050	0.773

*BC-PW: pine wood biochar microparticles, BC-PM: Pig manure biochar microparticles
.

Q_o and K_L are Langmuir constants for adsorption capacity and rate of adsorption, respectively. K_F is the adsorption capacity of the adsorbent and n is the favourability factor of the adsorption. b_T is the Temkin constant related to heat of sorption ($J\ mol^{-1}$) and A_T is the Temkin isotherm constant ($L\ g^{-1}$). q_m is the amount of DCF adsorbed onto per unit dosage of biochar ($\mu g\ g^{-1}$), q_m is the theoretical monolayer sorption capacity ($\mu g\ g^{-1}$) and β is the constant of the sorption energy ($mol^2\ J^{-2}$)

34

Table 3: Thermodynamic parameters for the adsorption of DCF onto biochar microparticles, BC-PW and BC-PM

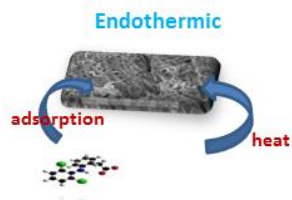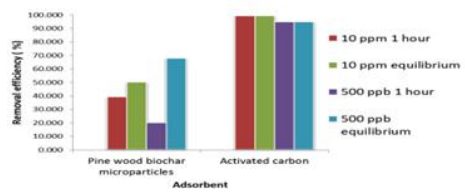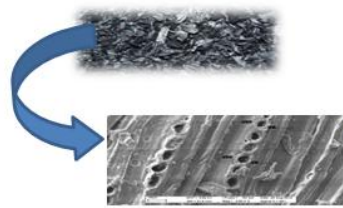| Adsorbents	Temperature (K)	Removal (%)	$\Delta G°$ (kJ/mol)	$\Delta H°$ (kJ/mol)	$\Delta S°$ (J/mol K)
	283	56.73	2.376		
	293	53.57	2.420		
BC-PW	298	52.93	2.442	1.130	-4.404
	303	50.10	2.464		
	313	47.27	2.508		
	323	30.13	2.552		
	283	94.61	-8.534		
	293	95.83	-8.696		
	298	97.04	-8.776	-3.970	16.13
BC-PM	303	98.68	-8.857		
	313	98.74	-9.018		
	323	98.80	-9.180		

*BC-PW : pine wood biochar microparticles, BC-PM : Pig manure biochar microparticles

35

Highlights

➤ Biochar (microparticles) were used for removal of diclofenac for the first time

➤ A maximum of 99.6% removal was observed for diclofenac with pig manure biochar

➤ Interface chemistry of adsorption was explained with kinetic studies and isotherms

➤ Thermodynamics of adsorption process was extensively studied

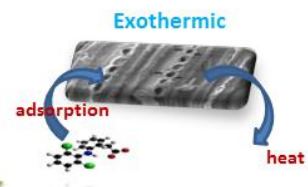➤ Effect of surface charges and functional groups on adsorption was studied
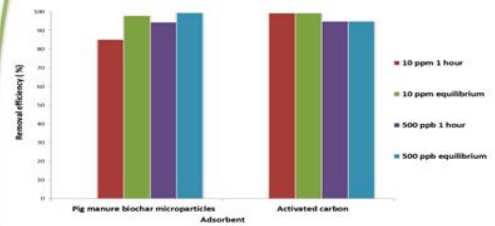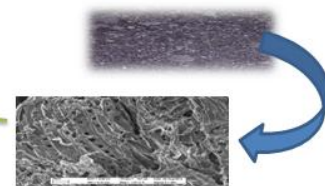
Pinewood Biochar

Pig manure Biochar

Diclofenac

Interface processes during adsorption

Removal efficiency [%]

10 ppm 1 hour
10 ppm equilibrium
500 ppb 1 hour
500 ppb equilibrium

Pine wood biochar microparticles — Activated carbon

Adsorbent

Removal efficiency [%]

10 ppm 1 hour
10 ppm equilibrium
500 ppb 1 hour
500 ppb equilibrium

Pig manure biochar microparticles — Activated carbon

Adsorbent

Endothermic

adsorption

heat

Exothermic

adsorption

heat